Atmos. Chem. Phys. Discuss., 11, 17245–17287, 2011
www.atmos-chem-phys-discuss.net/11/17245/2011/
doi:10.5194/acpd-11-17245-2011

Atmospheric Chemistry and Physics Discussions

Novel application of satellite and in-situ measurements to map surface-level NO_2 in the Great Lakes region

C. J. Lee[1], J. R. Brook[2], G. J. Evans[1], R. V. Martin[3,4], and C. Mihele[2]

[1]Southern Ontario Centre for Atmospheric Aerosol Research, Department of Chemical Engineering and Applied Chemistry, University of Toronto, Toronto, Ontario, Canada
[2]Air Quality Research Division, Science and Technology Branch, Environment Canada, Downsview, ON, Canada
[3]Department of Physics and Atmospheric Science, Dalhousie University, Halifax, Nova Scotia, Canada
[4]Harvard-Smithsonian Center for Astrophysics, Cambridge, MA, USA

Received: 12 March 2011 – Accepted: 31 May 2011 – Published: 21 June 2011

Correspondence to: C. J. Lee (colinj.lee@utoronto.ca)

Published by Copernicus Publications on behalf of the European Geosciences Union.

Abstract

Ozone Monitoring Instrument (OMI) tropospheric NO_2 vertical column density data were used in conjunction with in-situ NO_2 concentrations collected by permanently installed monitoring stations to infer 24 h surface-level NO_2 concentrations at 0.1° (~ 11 km) resolution. The region examined included rural and suburban areas, and the highly industrialised area of Windsor, Ontario, which is situated directly across the US-Canada border from Detroit, MI. Photolytic NO_2 monitors were collocated with standard NO_2 monitors to provide qualitative data regarding NO_z interference during the campaign. To test the accuracy of the OMI-inferred concentrations, two-week integrative NO_2 measurements were collected using passive monitors at 18 locations, approximating a 15 km grid across the region, for 7 consecutive two-week periods. When compared with these passive results, satellite-inferred concentrations showed an 18 % positive bias. The correlation of the passive monitor and OMI-inferred concentrations ($R = 0.69$, $n = 115$) was stronger than that for the passive monitor concentrations and OMI column densities ($R = 0.52$), indicating that using a sparse network of monitoring sites to estimate concentrations improves the direct utility of the OMI observations. OMI-inferred concentrations were then calculated for four years to show an overall declining trend in surface NO_2 concentrations in the region. Additionally, by separating OMI-inferred surface concentrations by wind direction, clear patterns in emissions and affected down-wind regions, in particular around the US-Canada border, were revealed.

1 Introduction

Nitrogen oxides (NO_x), composed of nitric oxide (NO) and nitrogen dioxide (NO_2) are an important family of atmospheric pollutants ($NO_x = NO + NO_2$). The main source of NO_x in Ontario, Canada is transportation, with a smaller component originating from electricity generation and industrial processes (MOE, 2008). Other sources of NO_x

ACPD
11, 17245–17287, 2011

include soil and lightning. NO_2 has been used as a marker for vehicle emissions and has thereby been associated with adverse human health effects (Brook et al., 2007; Jerrett et al., 2009; Clark et al., 2010; Lenters et al., 2010). In the province of Ontario, Canada, the government guideline exposure limit for NO_2 is 100 ppb averaged over 24 h and 200 ppb averaged over 1 h. Despite the association of NO_2 with adverse health outcomes, and its utility as a marker for traffic and/or combustion pollution, NO_2 monitoring networks remain sparse.

NO_2 is commonly measured by chemiluminescence (CL) monitors which work by reducing NO_2 to NO and measuring the light produced by titrating the NO with O_3. There are a number of methods for reducing the NO_2, the most common being a heated molybdenum surface, which becomes oxidized to MoO_2 and MoO_3 and must be periodically recharged. We will refer to this type of monitor as MoO. These monitors are known to suffer from interference due to other oxidized nitrogen species NO_z ($NO_z = HNO_3 + HONO + N_2O_5 + RONO_2 + \ldots$), since the heated molybdenum surface exhibits low selectivity (Steinbacher et al., 2007). This interference can especially be a problem in rural areas with low NO_2 concentrations and high NO_z due to aged air masses or high organic concentrations. Photolytically converted CL monitors do not suffer from this interference (Ryerson et al., 2000). These photolytic monitors operate on essentially the same principle as the MoO-CL monitors, however, the NO_2 is reduced by applying intense light at $\sim$420 nm which is specific to NO_2 and therefore is expected to produce almost no interference from other oxidized nitrogen species.

Due to the low relative per-monitor cost, NO_2 has also been measured using networks of passive monitors. For example, the networks have been used to assess human exposure to traffic related air pollution at high spatial resolution (Jerrett et al., 2009). These passive monitors consist of a chemically treated filter pad placed in a protective housing and exposed to ambient air for a period of time, usually two or more days. At the end of the sampling period, the filter is removed and the treatment is dissolved off the filter and analyzed using ion chromatography. Although the filters themselves are inexpensive, the method is labour intensive. As well, since there are

ACPD
11, 17245–17287, 2011

no pumps, the exposure, and therefore the collection efficiency, is influenced by local meteorology.

Beginning with the Global Ozone Monitoring Experiment (GOME) in 1995, satellite-based spectroscopic measurements of atmospheric NO_2 have been taken by a series of instruments (Bovensmann et al., 1999; Burrows et al., 1999; Levelt et al., 2006), The Ozone Monitoring Instrument (OMI), launched in 2004 aboard the Aura satellite, has provided near daily-global NO_2 column measurements at unprecedented spatial resolution. Many recent works have compared OMI NO_2 columns with measurements provided by in situ surface monitors (Kramer et al., 2008; Boersma et al., 2009), long-path surface measurements (Kramer et al., 2008) and in situ aircraft measurements (Bucsela et al., 2008). Recent validation studies indicate that biases in the satellite retrievals remain and must be addressed when interpreting the data (Hains et al., 2010; Herron-Thorpe et al., 2010; O'Byrne et al., 2010; Lamsal et al., 2010).

Lamsal et al. (2008) used GEOS-Chem, a global chemical transport model (CTM), to infer ground level concentrations from OMI NO_2 data and showed good agreement between OMI overpass measurements and 2 h averages from a large network of ground monitors over the continental US and Canada with a mean difference of −18 % (urban) to 11 % (rural) between OMI inferred concentrations and corrected surface monitor data during the summer and fall seasons. Other studies such as Boersma et al. (2009) and Russell et al. (2010) have examined spatial and temporal characteristics of NO_2 over smaller regions such as Israel and California. Additionally, satellite NO_2 measurements were found to agree well with surface-level column measurements taken by MAX-DOAS as part the BAQS-met campaign (Halla et al., 2011). These analyses indicate that insight into the spatial distribution of NO_2 at a regional-to-local scale on the Earth's surface can be achieved with satellite remote sensing.

These high resolution column density measurements have been combined with the GEOS-Chem model to constrain emissions inventories for the Eastern United States and Mexico (Boersma et al., 2008). Differences between these OMI-constrained top-down inventories and the US EPA National Emissions Inventory for 1999 (NEI99) were

ACPD
11, 17245–17287, 2011

further used to infer changes over time to emissions from specific sectors. This was possible due to the geographic separation of the different sectors' emissions and the fine spatial resolution of the OMI-constrained top-down inventories. OMI column data has also been used to help verify and develop a regional chemistry model with 15 km resolution around the state of California (Kim et al., 2009). The weekend effect was also observed and contrasted between different cities in California using OMI vertical column densities from multiple years averaged on a 0.025° (~ 3 km) grid (Russell et al., 2010).

The BAQS-met campaign was conducted in Southwestern Ontario, around the Windsor-Detroit area, from 1 June to 10 September 2007. The main goal of BAQS-met was to study the effects of transboundary air pollution and the Great Lakes meteorology on local air quality. The area was chosen due to its unique geography (i.e. frequent influence of lake breezes), proximity to the US-Canada border and local industry. Among a comprehensive suite of measurements, which have been described in other papers in this special issue (e.g., Levy et al., 2010), the campaign included a network of 18 passive NO_2 sites along with three photolytic NO_2 monitors operated by Environment Canada. The Ontario Ministry of the Environment (MoE) also operated 3 temporary MoO NO_2 monitors for the intensive campaign period (20 June to 11 July) in addition to the 3 permanent monitoring stations run by the MoE in the area. This diverse and relatively dense array of surface NO_2 measurements provided a unique opportunity to develop and evaluate OMI-derived surface NO_2 concentration estimates.

The objectives of the work in this paper are thus to develop an approach to use OMI tropospheric column data to estimate spatially resolved surface NO_2 concentrations at a regional-to-local scale and then to provide examples of the insights that can be gained regarding spatial and temporal patterns of surface NO_2 in the study region. OMI estimates of surface concentrations can provide a number of contributions to air quality research:

ACPD
11, 17245–17287, 2011

- to closely examine urban impacts on surrounding rural regions
- to improve estimates of chronic human and ecosystem exposure patterns
- to determine the overall uncertainty of the surface NO_2 concentration estimates provided at a reasonable resolution (e.g., 0.1° grid) over a reasonable time period (e.g., 2-week averages)
- to look at transboundary flow of NO_x which has been used as a combustion tracer when close to the source of combustion
- to gain insight into ways that OMI NO_2 can best be used to evaluate high-resolution air quality models, such as AURAMS, which was run for the study (Makar et al., 2010).

A major contribution of previous work in this area was the use of a CTM to estimate a surface-concentration-to-column-density ratio which was applied to satellite NO_2 columns for this purpose (Lamsal et al., 2008). We hypothesized that this ratio could be calculated using publicly available data from a network of permanent surface monitoring stations in place of the CTM, in regions with sufficient ground-based monitors. This approach has the advantage of simplicity since it is not dependent upon CTM runs, which are relatively costly and not available to all OMI data users. Another potential advantage to this method is the empirical nature by which it is calculated, making it less sensitive to the OMI data product used and eliminating the possibility of introducing additional biases from the model used in the inference process.

Because of the nature of the BAQS-met campaign setup, several important facets of our hypothesis could be examined and are reported in this paper. The estimated results were compared with passive NO_2 measurements obtained at 18 locations for each of 7 sampling periods. Since the passive sites were spaced as closely as 15 km and were not used to calculate the ratio (i.e., were independent), they were well suited for determining the accuracy of the estimated concentrations on a spatial scale not yet examined, across a variety of land-use types spanning from urban to rural locations.

ACPD
11, 17245–17287, 2011

The collocated conventional and photolytic NO_2 monitors allowed for quantification of the NO_z interference known to impact conventional measurements. Additionally, it was possible to examine the diurnal patterns in the interference and to assess the impact of these patterns on the comparison of the 14-day integrated passive NO_2 with the 14-day average OMI NO_2 based upon the midday overpasses. Finally, because of the additional rural chemiluminescence monitoring provided during the campaign, the value of these more spatially representative rural monitoring sites for improving the exploitation of the freely available OMI satellite observations could be highlighted.

To illustrate the potential applications of this methodology, ground-level NO_2 concentration maps determined from the OMI data were produced. These were then used to examine spatial and temporal variations in concentrations, providing new insights on air quality previously not available for the study region.

2 Measurements of Windsor area NO_2

2.1 Windsor and surrounding area

Windsor, Ontario, is located at the southwestern tip of the province of Ontario. It is bordered by the Detroit River on the west side and Lake St. Clair to the north, as well as Lake Erie several km to the south. This type of waterfront geography can have effects on NO_2 concentrations due to lake breezes (Arain et al., 2009). Across the Detroit river lies Detroit, MI. Both cities are known for their auto industry. The Windsor metropolitan area has a population of 323 000 and an area of 1023 km^2, while the City of Windsor has a population of 216 500 and occupies an area of 147 km^2 (Statistics Canada, 2006). Southeast Michigan, including Detroit-Warren-Flint, is the eleventh most populous combined statistical area in the US with a population of 5 300 000 and an area of 15 000 km^2 (US Census Bureau).

ACPD
11, 17245–17287, 2011

2.2 High-time resolution measurement by chemiluminescence

The Ontario Ministry of the Environment (MoE) operates a permanent monitoring network which includes 2 stations within Windsor and one in Chatham (Fig. 1). Due to their proximity to the campaign area, MoE permanent monitoring sites in Sarnia, at the Southern end of Lake Huron, and London, approximately 150 km Northeast of Windsor, were also included (Fig. 2). As well, during the intensive campaign period (20 June–10 July 2007) 3 additional chemiluminescence (CL) monitors were set up at Harrow and Ridgetown, on the North shore of Lake Erie approximately 40 km and 100 km from Windsor, respectively, and on Pelee Island, a 42 km^2 island approximately 50 km Southeast of Harrow in Lake Erie (Fig. 1). The monitors operated by MoE were Thermo TE42C instruments which provide NO, NO_2 and NO_x. Measurements were averaged to 1 h.

To evaluate the potential interference from non-NO_2 oxidized nitrogen species (Steinbacher et al., 2007; Ordóñez et al., 2006; Lamsal et al., 2008), 3 CL monitors (TE42C and TE42CTL) were deployed by Environment Canada for the duration of the campaign (1 June 2007 to 11 September 2007). These CL monitors were each equipped with a photolytic converter (Droplet Measurement Technologies, blue light converter) and an external molybdenum converter. By selecting ambient air, photolytically converted air, or molybdenum converted air, true NO_2 could be reported by subtracting NO from the measured post-conversion NO and applying the conversion efficiency of NO_2 to NO. One minute concentrations for NO, NO_2 and NO_y ($NO_y = NO_x + NO_z$) were provided by running a 1 min cycle with the three above channels and 2 internal zeros.

It is important to highlight that the method for measuring NO_y is exactly the same as the method commonly used for measuring NO_2 with the exception that in traditional atmospheric NO_2 monitoring, the converter is internal to the monitor. The NO_z interference in MoO NO_2 measurements is therefore a product of the conversion efficiency of the constituent species of NO_z as well as their respective line loss parameters (HNO_3 is particularly noted for line losses, Steinbacher et al., 2007). In the NO-NO_2-NO_y setup

ACPD
11, 17245–17287, 2011

used for measuring the interference, the MoO converter was applied before the sampling line and NO_y measurement was dependent only on the conversion efficiencies of the species.

2.3 Measurement by passive monitor

A network of passive NO_2 monitors was deployed at 18 locations (Fig. 2). These sites were part of the Mesonet study (Levy et al., 2010) and were chosen to closely match the Environment Canada Global Environmental Multiscale model (Makar et al., 2010) meteorological forecast 15 km model grid in the region (every grid point where possible, alternate grid points in other locations). In some cases the need to access the monitors on a regular basis caused small deviations from the model grid. Weatherproof housings were anchored to the Mesonet towers at the sampling sites. These housings were designed to allow ambient air contact with the monitors while keeping out rain.

Further, since the filters needed to be collected for analysis and replaced with fresh samplers manually, site locations were selected with the criterion that all sites could be reached in a single day. The intention was to provide consistent sampling period start and end dates across all sampling periods. However, this was not always possible and some sites saw collection and replacement up to two days before others, although most sites were collected and replaced on the same day in most cases. In total, there were 115 passive samples collected: the first 6 periods had 17 simultaneous sampling sites and the final period had 13 sampling sites. On average, 70 % of the filters were collected on a single day, thus maximizing temporal overlap for the two-week period. For sampling periods 1 and 3 through 7, all filters were collected within a 2 day period; for sampling period 2, all filters were collected within a 2 day period, except one filter which was collected 2 days later than the first.

Paired filters were deployed at each sampling location to ensure data quality and consistency of results. Collocated filters were checked for consistency and if values differed by more than 10 % the two measured concentrations were subjected to additional quality assurance checks to improve the IC results and, if acceptable (within

ACPD
11, 17245–17287, 2011

20 %), averaged. In the case of a known source of error, one filter was rejected and the site value was reported from only the good filter. Multiple unexposed filters, carried to and from the sampling locations during the campaign, were used for background/blank correction.

2.4 Satellite remote sensing

The Earth Observing System (EOS) Aura satellite which is in a sun-synchronous orbit with north-south Equator crossing of 13:45 LT (Levelt et al., 2006). OMI is carried aboard the Earth Observing System with a wide field-of-view and sun-synchronous orbit, the instrument was intended to achieve daily coverage across most of the globe, with some equatorial areas receiving only every-other-day measurements. The sensor observes 60 pixels which together cover a swath 2600 km wide, perpendicular to the direction of travel. The satellite travels at approximately 7 km s^{-1} ground speed and each exposure is roughly 2 s long, resulting in each row covering 13 km on the ground in the along-track direction. Across track, pixels are 24 km wide at nadir, but due to geometry, nearer the edge of the swath, pixels can be as wide as 150 km. Recently, obstruction of parts of the sensor has limited measurements slightly, removing as many at 18 pixels out of the 60.

Two commonly used, publicly available data products generated from the raw data collected by OMI are: the Standard Product (SP) provided NASA and the DOMINO Product provided by the Tropospheric Emissions Monitoring Internet Service (TEMIS) (Lamsal et al., 2010). Both data products begin by using the DOAS algorithm to fit the absorption spectrum of NO_2 to the measured spectrum of backscattered 365 to 500 nm solar radiation (Boersma et al., 2007). The contribution of stratospheric NO_2 is then removed (Bucsela et al., 2006; Boersma et al., 2007). The air mass factor (AMF) corrects for viewing geometry and light-scattering interferences such as clouds and aerosol particles. This AMF is applied to convert the measured slant columns into tropospheric vertical column densities. It is these corrections that introduce the most uncertainty in the reported vertical columns over polluted areas (Boersma et al., 2007, 2004; Martin et al., 2002).

ACPD
11, 17245–17287, 2011

The use of in situ data to determine the surface-to-column NO_2 relationship makes this analysis insensitive to potential bias in the OMI NO_2 data. Starting with the DOMINO product, a tropospheric slant column destriping process was used to remove scan-angle dependent bias (Celarier et al., 2008; Lamsal et al., 2010), using a 24 h history to compute single-scan position biases. Pixels with cloud radiance fractions greater than 0.3 were rejected, as were pixels near the edge of the swath (width > 50 km). The resulting vertical column densities easily identified the urban areas as major NO_2 sources (Fig. 2).

Whereas in situ measurements are true surface measurements, OMI tropospheric NO_2 vertical column density measurements include both the surface-level NO_2 and its vertical distribution through the tropospheric column. This distribution depends on the chemical lifetime of NO_x, the partitioning of NO_x into NO and NO_2, layering of the atmosphere and the dispersion of NO_x during vertical mixing. Surface-level NO_2 concentrations (S) have been inferred from OMI tropospheric vertical column densities (Ω) by comparison of surface-level NO_2 concentrations ($\overline{S}$) and vertical column densities ($\overline{\Omega}$) calculated using the GEOS-Chem global CTM (Lamsal et al., 2008):

$$S = \frac{\overline{S}}{\overline{\Omega}} \times \Omega \quad (1)$$

In order to obtain surface concentrations without the use of a CTM, we determined the average ratio of column to surface concentration ($\overline{\Omega}$ to $\overline{S}$) for each OMI overpass over the region using the high-time resolution surface monitors.

To account for the larger fractional contribution of the free troposphere in areas with low surface concentrations, all pixels (after filtering) in the region contained by the boundary of Fig. 2 were sorted by column density for each overpass. The lowest decile value (i.e., the value separating the bottom 10 % of the data from the remaining 90 % of pixels) was subtracted from every pixel in the overpass. This allowed for the free-tropospheric component to be accounted for, while limiting sensitivity to the uncertainty of any single pixel. The mean value of the free-tropospheric column during the

ACPD
11, 17245–17287, 2011

campaign period was 0.8×10^{15} molec cm^{-2}. This process did result in negative (i.e., below detection) values, but they were typically small and constrained to the northernmost areas of the region.

Each single-pixel measurement carries with it an uncertainty due to the spectral fitting, surface albedo, cloud cover and air mass factor. This uncertainty can reach up to 40 % in heavily polluted areas (Boersma et al., 2007), including the locations of some of the high-time resolution in situ monitors used to calculate the surface-to-column ratio. In addition to this, an OMI pixel is an average over a large area on the surface of the Earth while the in situ monitors measure at a specific location which is not necessarily representative of the entire pixel area against which is being compared. It was therefore necessary to generate an average surface-to-column ratio for the entire region by averaging the ratios observed at several surface monitoring stations. Implicit to this approach was the assumption that this ratio varies temporally (i.e., day-to-day) but not spatially across the region on any given day. The error in this assumption is discussed below.

To generate the inferred surface concentration map for a given overpass, every pixel from the overpass (Ω in Eq. 1), minus the free-tropospheric contribution, was multiplied by this average ratio ($\overline{\frac{S}{\Omega}}$ in Eq. 1) to provide a region-wide snapshot of surface NO_2 concentrations at overpass time. This procedure was analogous to Eq. (4) from Lamsal et al. (2008), which also accounts for the contribution of the free troposphere. Equation (4) from Lamsal et al. (2008) also provides higher resolution than the available GEOS-Chem $2^\circ \times 2.5^\circ$ resolution using a ratio of local OMI columns to the average OMI column for the entire grid cell. This suggests that by using a single ratio for the entire region for each overpass, an error of up to ± 35 % is introduced in rural areas.

For comparison of OMI column densities and surface concentrations with long-term time-averaged passive monitor results, OMI measurements were resampled on a $0.1^\circ \times 0.1^\circ$ grid. Each grid cell was then given a weight proportional to the inverse of the area of the pixel which contained that grid cell. This had the effect of giving near-nadir pixels higher weight than pixels closer to the swath edge. These regridded

ACPD
11, 17245–17287, 2011

measurements were then averaged over two weeks using these weights, providing a long-term average to compare with in situ passive monitor measurements.

3 Results and discussion

3.1 Characterising surface NO_2

3.1.1 High-time-resolution measurements

NO_2 concentrations were found to vary both spatially and temporally. The hourly and daily concentrations of NO_2 showed moderate to weak correlations between the sites over the duration of the campaign for both hourly and daily average measurements (Table 1). Ridgetown showed a relatively high correlation with the urban sites, which was surprising because Ridgetown is over 100 km from the urban and industrial centres of Windsor. However, the Ridgetown measurement site was 5 km from highway 401, a major provincial highway in the region which terminates in Windsor, at a large roadway which leads directly to the Ambassador Bridge border crossing. This relatively strong correlation despite the spatial separation implied that 401 traffic was an important source at both sites, possibly due to commercial vehicle traffic.

NO_2 concentrations varied diurnally and day-to-day at both the urban (Windsor) and rural (Harrow, Bear Creek) sites (Fig. 3). Peak concentrations for Windsor occurred between 06:00 and 10:00 a.m. (local standard time) on most days, while these morning rush-hour peaks were sometimes delayed at the rural sites downwind. When averaged over a longer period of time, such as a week, NO_2 concentrations varied much more spatially than temporally (Table 2). The largest between-site ratio in the median weekly concentration was over 4 whereas the largest ratio between maximum and minimum weekly concentrations at a single site was less than 2. In contrast, daily averages varied about as much at a given site as they did between sites. This indicated that spatial distributions remain fairly stable over the region, even though local events may briefly

ACPD
11, 17245–17287, 2011

increase the spatial heterogeneity. This result is important for high spatial resolution interpretation of satellite remote sensing data because these methods take advantage of differences in the daily footprint of the instrument overpass to extract long-term patterns in spatial air pollution distributions.

3.1.2 Passive monitor results

Campaign average NO_2 measurements recorded at the passive monitoring sites ranged from a minimum site average of 3.3 ppb (rural) to a maximum of 18.8 ppb (urban). The passive monitors also revealed that over the long-term the magnitude of the spatial variability was greater than the magnitude of the differences between time periods at a given location. This is exemplified in Fig. 4, comparing the concentrations measured at each location for sampling period 6 (7 August to 21 August) to the campaign average concentration at each sampling site. In fact, the minimum correlation coefficient between a single sampling period and the campaign average was observed during period 6 ($R = 0.97$); all other sampling periods correlated with campaign averages with $R > 0.98$, with a slope near 1. The maximum ratio between minimum and maximum two-week average NO_2 concentrations at any given site was 1.8, while the ratio between the highest site median value and the lowest site median value was 6.4. This result is consistent with the findings presented in Sect. 3.1.1, that long term spatial patterns remain relatively stable compared with the differences in concentration across the region. This also highlights the potential that midday satellite observations averaged over multiple days can have in capturing the spatial pattern.

A passive monitor was located at Harrow for the first 3 two-week sampling periods (1 June 2007 to 10 July 2007) as well as a photolytically converted CL monitor for the entire campaign and a MoO-CL monitor for the intensive campaign (20 June to 10 July). Bear Creek had a passive monitor for the remaining 4 periods (11 July 2007 to 4 September 2007) along with both photolytically and MoO converted CL monitors. As well, the permanent MoE site (molybdenum converted NO_2), Windsor West, had a passive monitor. The passive monitors were in reasonably good agreement with the

ACPD
11, 17245–17287, 2011

collocated CL monitors (Fig. 5a). The average absolute difference between the passive and the MoO CL and the photolytic CL were 11 % and 15 %, respectively. The overall slope of the relationship was 1.04.

Passive monitors provide time integrated averages while OMI only measures once daily, between 12:00 and 14:00 LT at this latitude. It was therefore important to understand how the average NO_2 values just around OMI overpass times (12:00 to 14:00 LT each day) relate to concentrations averaged over the two-week timescale of the passive monitor measurements. Although the slope was, as expected, substantially higher since the midday NO_2 values were lower than daily averages, the correlation remained strong (Fig. 5b). Similar results were obtained when daily average CL data were compared to midday averages from the same monitors. This indicated that, with a suitable correction factor, OMI overpass averages could be adjusted so as to be representative of long-term integrated averages.

3.2 NO_z interference

Much of the NO_2 monitoring data available are taken by MoO converted CL monitors. As indicated above, these converters are not specific to NO_2, suffering from interference from other oxidized nitrogen species (NO_z). Previous studies have reported MoO-converted CL NO_2 measurements to be as much as 2.3 times higher than simultaneous photolytically-converted CL measurements during summer months in a rural setting (Steinbacher et al., 2007). Quantifying this interference is important for the interpretation of satellite remote sensing data, which are specific to NO_2 and provides averages over a large area on the Earth's surface. Often satellite measurements are compared to rural monitors to ensure that the in situ data are representative of a wide local area and not affected by local sources (Lamsal et al., 2010). It is these rural monitors where the interference is expected to be the largest (Boersma et al., 2009).

In this study photocatalytic and heated molybdenum converted chemiluminescence monitors were collocated to evaluate the effects of NO_z interference on the molybdenum converted measurements. All data was averaged to 1 h resolution, which

ACPD
11, 17245–17287, 2011

corresponds with the resolution of the publicly available data for the permanent CL monitoring sites. At the Bear Creek (BC) site, the molybdenum-converted CL monitor hourly concentration was found to be 45 % (± 3%) higher, on average, than the photolytically-converted CL. The MoO measurements correlated strongly with the photolytic ($R = 0.96$, $n = 1472$), with a slope of 1.05 and an offset 0.65 ppb. This offset was responsible for the apparently large relative difference as the average NO_2 concentration for the site was only 2.9 ppb. When the difference between the two monitors was compared with NO_z measurements taken by the photolytic monitor (Fig. 6), there was only a weak correlation ($R = 0.26$, $n = 1464$) with a slope of 0.11 and an offset similar to that found when comparing the two sets of NO_2 measurements. Since the only difference between NO_z as measured by the photolytic monitor and NO_2 measured by the molybdenum converted monitor was the point of conversion, the most likely explanation for the low slope and high offset is inlet deposition of NO_z species. That is, about 90 % of the NO_z is deposited on the way to the MoO CL monitor, but some of this is later released, resulting in NO_z interference even in the absence of detectable ambient NO_z. In the 3 locations where NO_z measurements were available, mean NO_z between noon and 1400 EDT were found to be low (2.62 and 3.22 for rural locations and 2.62 for urban), indicating that NO_z concentrations (and therefore NO_z interference) remain low across the entire campaign region.

The interference by NO_z did show a diurnal trend (Fig. 7). The median ratio of the MoO-CL to photolytic-CL monitor data was around to 1.15 for hours between midnight and 08:00 a.m., with a rise towards the afternoon and a maximum of 1.97 for 01:00 p.m. LST, then back down to 1.0 from 06:00 p.m. to midnight. Because of the rural location chosen for this comparison, the high midday ratio was partly due to the low NO_2 concentrations observed around midday – while the ratio of the MoO-CL to the photolytic-CL measurements was almost 2, the median difference between the monitors was only 0.9 ppb for the same time (01:00 p.m. local). This is largely due to the relatively low NO_2 concentrations at the monitoring location. When only hours for which the average photolytic NO_2 concentration was greater than or equal to 1 ppb

ACPD
11, 17245–17287, 2011

were considered, this 01:00 p.m. median ratio is reduced to 1.53. Thus, the interference by NO_z could cause significant uncertainties (up to 97 %) if the OMI data were compared only to midday MoO CL in situ concentration data for rural areas. However, the goal of this study was to compare long-term average NO_2 concentrations with OMI measurements over a range of environments including rural areas with low concentrations and urban and industrial areas with higher NO_2 concentrations. Since all of the permanent monitoring locations (with MoO converted CL monitors) were in urban settings with higher average NO_2 levels, this 0.9 ppb median difference was deemed to be acceptable. Thus it was concluded that NO_2 data from the MoO-CL and photolytic-CL monitors could be combined and used for comparison with the OMI or passive monitor data.

3.3 Satellite observations

3.3.1 Comparison with in situ passive measurements

Twenty-four hour surface NO_2 concentrations were estimated from OMI column data using the CL monitor data in conjunction with Eq. (1). The accuracy of the resulting ground-level spatial maps derived from this approach was evaluated by comparison with the passive monitoring data from the 17 sites. Without using Eq. (1), inverse-area-weighted averages of OMI tropospheric NO_2 vertical column measurements showed moderate correlation ($R = 0.52$, $n = 115$) with passive monitor concentrations. This was considered the baseline correlation, against which the inference method could be evaluated.

Qualitatively, OMI-inferred concentrations showed a similar geographical pattern to the passive monitoring network (Fig. 8). The highest concentrations were observed in the Detroit and Windsor urban areas with moderate values observed along the US-Canada border between Lake St. Clair and Lake Huron. The geographical pattern observed in the OMI-inferred NO_2 concentrations also follows the distribution of emissions sources with many of the NO_2 point sources, as reported by the Environment Canada

ACPD
11, 17245–17287, 2011

National Pollutant Release Inventory and the United States Environmental Protection Agency. Figure 8 shows that many sources are clustered around the Detroit-Windsor urban area and along the border between Lake St. Clair and Lake Huron.

The procedure for calculating surface NO_2 from OMI columns was performed in two ways: once using the campaign-only NO_2 data in addition to the permanent MoE monitoring sites (7 sites total), and once using only the permanent MoE monitoring sites (5 sites). Correlation between OMI measurements and passive measurements improved from 0.52 using raw OMI NO_2 columns to 0.69, with a slope of 1.18, using the OMI inferred surface concentrations (Fig. 9). Interestingly, when only the MoE permanent monitoring stations were used, a correlation of 0.66 was obtained, but the slope increased from 1.18 to 1.32. The higher slope obtained when using only the five permanent MoE sites is attributed to their locations near NO_x sources in urban sites. These in-situ NO_2 measurement are expected to be less representative of the overall pixel area whose average column is measured by OMI.

The surface-to-column ratios used to calculate OMI-inferred surface-level NO_2 concentrations varied somewhat across the 7 CL monitor sites with the lowest average ratio being 0.36 ppb/1 × 10^{15} molec cm^{-2} (i.e., 8.6 × 10^{-6} cm^{-1}) at the Environment Canada Bear Creek site and the maximum average ratio being 1.66 ppb/1 × 10^{15} molec cm^{-2} (4.0 × 10^{-5} cm^{-1}) at the MoE Chatham site. It is worth noting that the inverse of these surface-to-column ratios represents a characteristic height (H) that varied from 250 to 1160 m. This metric provides a measure of the vertical extent of the NO_2, assuming that the ground based measurement was representative of the OMI pixel.

In the case of the MoE Chatham site, the most likely local emission source is on-road vehicles. The urban area of Chatham itself is small (~ 5 km in diameter or 20 km^2) and surrounded by rural areas. Thus, the surface NO_2 concentration within Chatham tends to be higher than that in the surrounding rural region. As a result, measurement at this MoE site is less representative of the area over which the OMI measurements are averaged, which is a minimum of 300 km^2. Since most of the area included in the OMI pixel footprint is the surrounding rural area, as opposed to the urban area of Chatham,

ACPD
11, 17245–17287, 2011

the high in situ concentration in Chatham and the low overall column density would result in a high surface-to-column ratio, as observed.

In the region upwind of the Bear Creek site there are a number of stack emissions sources (Fig. 8). Thus, NO_2 in this rural region has a higher potential to be above ground, compared to the vehicle emissions in Chatham. The low surface-to-column ratio determined for this site reflects this situation. The hypothesis of lofted NO_2 in this rural area is also borne out by the inferred NO_2 at the location of the passive monitor 18 km to the north of the Bear Creek monitoring site. At this location, OMI inferred concentrations were 5.4 ppb higher, on average, than the concentrations measured by this passive monitor.

These two extreme situations highlight some of the limitations of this approach. Using a CTM to provide a better estimate of the free-tropospheric column and applying Eq. (4) of Lamsal et al. (2008) could potentially lead to improvements in the surface NO_2 estimates, especially in rural areas. Another possible approach would be to empirically determine a spatially varying surface-to-column ratio, by fitting a polynomial surface to interpolate the measured point values. However, for this approach to work, a higher density in situ monitoring network would be required to capture the variability and to account for the uncertainty in each individual surface-to-column measurement. The simplest step towards improving the inference of ground-based NO_2 from OMI data would be to increase the proportion of NO_2 monitoring locations at rural sites.

3.3.2 Temporal patterns

Temporal patterns in the OMI data and inferred ground-based concentrations were explored to illustrate the application of this methodology. The patterns examined included the variation in inferred concentrations across the region over four years, and the seasonality in the surface-to-column ratio. Over a span of 4 yr, using only the 5 permanent MoE monitoring stations, the seasonal average surface-to-column ratio was found to vary from a minimum of 0.81 ppb/1×10^{15} molec cm^{-2} ($H = 525$ m) in the autumn and a maximum of 2.0 ppb/1×10^{15} molec cm^{-2} ($H = 210$ m) in the winter (Table 3). No

ACPD
11, 17245–17287, 2011

significant relationship with characteristic height was found for any meteorological variable. However, Lake Erie's water temperature normally follows a very similar seasonal trend, with winter and spring (December through May) having lower lake temperatures than summer and autumn (June through November) (NOAA, 2010). Therefore, it appears that higher lake temperatures in the summer and autumn may be driving the vertical mixing of NO_2 in the region, as seen in the seasonal pattern in characteristic height.

In order to verify the validity of the surface NO_2 procedure developed from the BAQS-Met period for use over longer time spans, we calculated two week average OMI-derived surface-level NO_2 concentrations using only 4 of the 5 available permanent MoE monitoring sites, retaining the last site for evaluation. For this purpose, two week averages were calculated for both in situ CL measured NO_2 concentration at the hold-back site and OMI-inferred NO_2 concentration for the nearest 0.1° grid cell. This procedure was done for every 2-week period from January 2005 to December 2009, randomly changing which site was held back each time. Surface inferred OMI concentrations showed a stronger correlation ($R = 0.68$, Fig. 10) with in-situ CL-measured 2-week averages than OMI column values ($R = 0.61$). This provides confidence that the inference method is applicable to other periods (i.e., not just the summer 2007 BAQS-met campaign period), continuing to add skill to the estimates of surface NO_2. This improvement (i.e. increase in correlation) is largely due to a few specific periods which appear to benefit the most from the inference method. These periods all occurred between the months of November and March, and were observed across all 5 yr. These months tend to have more pixels excluded due to clouds and snow. Column averages calculated from fewer overpasses would suffer more from day-to-day variations in the surface-to-column ratio, whereas our method removes this influence from each overpass. Furthermore, OMI NO_2 retrievals are expected to be biased over snow (O'Byrne et al., 2010); our approach empirically corrects for that bias.

ACPD
11, 17245–17287, 2011

As an illustrative example, Fig. 11 provides regional snapshots of OMI-inferred surface NO_2 concentrations for 4 yr. From 2006 to 2009, OMI-inferred NO_2 in the region displayed a slow decline in and around the industrial areas on both sides of the border overall, with a sudden drop in the summer of 2009. This decrease in regional NO_2 concentrations may have coincided with a drop in manufacturing in the area during the economic slowdown after the fall of 2008. Concentrations over the West end of Lake Erie remained fairly stable in comparison with concentrations onshore nearby, indicating that meteorologically driven dispersion of NO_2 remained constant over 3 of the 4 yr in question.

3.3.3 Spatial patterns

Figure 12 shows average OMI inferred surface NO_2 concentrations for the entire 2007 year separated by wind direction. It is important to acknowledge the implicit assumption that exclusion of some days due to clouds does not introduce any bias in the maps. The long term comparison using the leave-one-out approach indicates that this is true, in general. It is possible, however, that, when separating overpasses by wind direction, we are exposing systematic errors which are masked by combining all overpasses. That is, if cloudy days from the southeast direction are cleaner than clear days and if cloudy days from the southwest direction are more polluted than clear days, by combining the days from both of these directions the errors cancel each other out. Also, it should be pointed out that the same single surface-to-column ratio calculated for the BAQS-met study area was applied across the entire range of the maps. The error introduced by this assumption may grow as the distance from the original points of calculation grows and therefore what appear to be large differences between wind directions around the Toronto area (Northeast corner of the maps) could in fact be errors introduced by this assumption.

Figure 12d includes OMI measurements when the wind was blowing from due East to due South directions. This quadrant was particularly important to the study of the region because it illustrated the impact of easterly airflows nearly perpendicularly

ACPD
11, 17245–17287, 2011

across the Canada-US border at Windsor-Detroit, thus highlighting any NO_x emissions sources on the Canadian side. The sharpness of the boundary can be observed on the NW shore of Lake St Clair (marked in fuchsia in Fig. 12d): over the lake the column measures approximately half those immediately adjacent the lake on the NW shore.

In order to more clearly see the effects of wind direction on surface level NO_2 concentrations, Fig. 13 shows the difference between the average concentration grouped by wind direction and the annual average concentration (all wind directions). Overall, NO_2 concentrations were higher when the wind blew from the SE and SW. Looking at the campaign area, the area between Lake Erie and Lake St. Clair (circled in red in Fig. 13c,d), a different pattern emerges: the area remains relatively unaffected by wind direction except for markedly elevated NO_2 concentrations across the entire region, as well as the west end of Lake Erie, when the wind blows from the NW. Good agreement between the satellite-derived, wind-direction-dependent concentrations and in-situ, wind-direction-dependent concentrations was also found.

It should also be possible to discern areas of intense emissions from the difference maps. Indeed, the core of Detroit/Windsor, near the Ambassador Bridge over the Detroit River, is consistently found to be a boundary between below average and above average concentrations, for all wind directions (Fig. 13). Another area of interest is the area to the north of Lake St. Clair, just south of Sarnia where a large power generation station is situated in Ontario, as well as several emissions sources on the US side. Outflow can be seen from Cleveland, on the south side of Lake Erie, especially over the lake when wind flows from the SW.

4 Conclusions

We have shown that utilization of empirically calculated surface-to-column ratios in conjunction with OMI satellite NO_2 column measurements can provide reasonable long-term surface concentrations at a regional-to-local scale ($\sim$ 11 km resolution). The approach leads to useful information on spatial and temporal variations in surface NO_2

ACPD
11, 17245–17287, 2011

without requiring a computationally expensive CTM, if sufficient in situ measurements are available for the region. This approach has the advantage of providing an empirical correction for the bias in OMI NO_2 retrievals.

We showed that this method can be exploited to examine the extent of outflow of urban air pollution at a regional scale. Significant contributions to rural NO_2 pollution in Southwestern Ontario were displayed when wind flowed from the NW direction, due to outflow from the Windsor-Detroit area. These examples have shown how future work using these types of maps in qualitative and quantitative analyses such as population exposure assessment and model evaluation, could be conducted.

NO_z interference was quantified using collocated monitors and it was shown that intake line adsorption and desorption contribute to both the magnitude of this interference and its temporal smoothing. Because of this smoothing, the effects of high midday ratios of $(NO_2)_m/NO_2$, driven largely by low midday NO_2 values, can be mitigated by using whole-day averages.

It should be noted that, although the long term results were calculated using only the urban monitoring stations permanently maintained by the Ontario Ministry of the Environment, comparison of OMI inferred NO_2 concentrations to campaign passive monitoring data showed a slope much closer to one when rural monitoring locations were also included. This was attributed mainly to the situation of permanent monitoring stations near sources, making these point sources less representative of the entire spatial footprint represented by a single OMI pixel measurement of the same location. It may be sensible, therefore, in future to allocate more monitoring resources to rural areas, where spatial distribution of NO_2 is less heterogeneous, to aid in interpretation of satellite results, which can yield significant insights into regional scale air quality.

Acknowledgements. We would like to thank the Canadian Foundation for Climate and Atmospheric Sciences for funding for this study and the Ontario Ministry of the Environment for providing NO_2 data and support for the BAQS-met campaign.

ACPD
11, 17245–17287, 2011

References

Arain, M. A., Blair, R., Finkelstein, N., Brook, J., and Jerrett, B.: Meteorological influences on the spatial and temporal variability of NO_2 in Toronto and Hamilton, Can. Geogr.-Geogr. Can., 53, 165–190, 2009. 17251

Boersma, K., Eskes, H., and Brinksma, E.: Error analysis for tropospheric NO_2 retrieval from space, J. Geophys. Res.-Atmos., 109, D04311, doi:10.1029/2003JD003962, 2004. 17254

Boersma, K. F., Eskes, H. J., Veefkind, J. P., Brinksma, E. J., van der A, R. J., Sneep, M., van den Oord, G. H. J., Levelt, P. F., Stammes, P., Gleason, J. F., and Bucsela, E. J.: Near-real time retrieval of tropospheric NO_2 from OMI, Atmos. Chem. Phys., 7, 2103–2118, doi:10.5194/acp-7-2103-2007, 2007. 17254, 17256

Boersma, K. F., Jacob, D. J., Bucsela, E. J., Perring, A. E., Dirksen, R., van der A, R. J., Yantosca, R. M., Park, R. J., Wenig, M. O., Bertram, T. H., and Cohen, R. C.: Validation of OMI tropospheric NO_2 observations during INTEX-B and application to constrain NO_x emissions over the Eastern United States and Mexico, Atmos. Environ., 42, 4480–4497, doi:10.1016/j.atmosenv.2008.02.004, 2008. 17248

Boersma, K. F., Jacob, D. J., Trainic, M., Rudich, Y., DeSmedt, I., Dirksen, R., and Eskes, H. J.: Validation of urban NO_2 concentrations and their diurnal and seasonal variations observed from the SCIAMACHY and OMI sensors using in situ surface measurements in Israeli cities, Atmos. Chem. Phys., 9, 3867–3879, doi:10.5194/acp-9-3867-2009, 2009. 17248, 17259

Bovensmann, H., Burrows, J. P., Buchwitz, M., Frerick, J., Noel, S., Rozanov, V. V., Chance, K., and Goede, A. P. H.: SCIAMACHY: mission objectives and measurement modes, J. Atmos. Sci., 56, 127–150, 1999. 17248

Brook, J. R., Burnett, R. T., Dann, T. F., Cakmak, S., Goldberg, M. S., Fan, X., and Wheeler, A. J.: Further interpretation of the acute effect of nitrogen dioxide observed in Canadian time-series studies, J. Expo. Sci. Env. Epid., 17, S36–S44, doi:10.1038/sj.jes.7500626, 2007. 17247

Bucsela, E., Celarier, E., Wenig, M., Gleason, J., Veefkind, J., Boersma, K., and Brinksma, E.: Algorithm for NO_2 vertical column retrieval from the Ozone Monitoring Instrument, IEEE T. Geosci. Remote, 44, 1245–1258, doi:10.1109/TGRS.2005.863715, 2006. 17254

Bucsela, E. J., Perring, A. E., Cohen, R. C., Boersma, K. F., Celarier, E. A., Gleason, J. F., Wenig, M. O., Bertram, T. H., Wooldridge, P. J., Dirksen, R., and Veefkind, J. P.: Comparison of tropospheric NO_2 from in situ aircraft measurements with near-real-

ACPD
11, 17245–17287, 2011

time and standard product data from OMI, J. Geophys. Res.-Atmos., 113, D16S31, doi:10.1029/2007JD008838, 2008. 17248

Burrows, J., Weber, M., Buchwitz, M., Rozanov, V., Ladstatter-Weissenmayer, A., Richter, A., DeBeek, R., Hoogen, R., Bramsteadt, K., Eichmann, K., Eisinger, M., and Perner, D.: The Global Ozone Monitoring Experiment (GOME): mission concept and first scientific results, J. Atmos. Sci., 56, 151–175, 1999. 17248

Celarier, E. A., Brinksma, E. J., Gleason, J. F., Veefkind, J. P., Cede, A., Herman, J. R., Ionov, D., Goutail, F., Pommereau, J. P., Lambert, J. C., van Roozendael, M., Pinardi, G., Wittrock, F., Schönhardt, A., Richter, A., Ibrahim, O. W., Wagner, T., Bojkov, B., Mount, G., Spinei, E., Chen, C. M., Pongetti, T. J., Sander, S. P., Bucsela, E. J., Wenig, M. O., Swart, D. P. J., Volten, H., Kroon, M., and Levelt, P. F.: Validation of Ozone Monitoring Instrument nitrogen dioxide columns, J. Geophys. Res., 113, D15S15, doi:10.1029/2007JD008908, 2008. 17255

Clark, N. A., Demers, P. A., Karr, C. J., Koehoorn, M., Lencar, C., Tamburic, L., and Brauer, M.: Effect of early life exposure to air pollution on development of childhood asthma, Environ. Health Persp., 118, 284–290, doi:10.1289/ehp.0900916, 2010. 17247

Hains, J. C., Boersma, K. F., Kroon, M., Dirksen, R. J., Cohen, R. C., Perring, A. E., Bucsela, E., Volten, H., Swart, D. P. J., Richter, A., Wittrock, F., Schönhardt, A., Wagner, T., Ibrahim, O. W., van Roozendael, M., Pinardi, G., Gleason, J. F., Veefkind, J. P., and Levelt, P.: Testing and improving OMI DOMINO tropospheric NO_2 using observations from the DANDELIONS and INTEX-B validation campaigns, J. Geophys. Res.-Atmos., 115, D05301, doi:10.1029/2009JD012399, 2010. 17248

Halla, J. D., Wagner, T., Beirle, S., Brook, J. R., Hayden, K. L., O'Brien, J. M., Ng, A., Majonis, D., Wenig, M. O., and McLaren, R.: Determination of tropospheric vertical columns of NO_2 and aerosol optical properties in a rural setting using MAX-DOAS, Atmos. Chem. Phys. Discuss., 11, 13035–13097, doi:10.5194/acpd-11-13035-2011, 2011. 17248

Herron-Thorpe, F. L., Lamb, B. K., Mount, G. H., and Vaughan, J. K.: Evaluation of a regional air quality forecast model for tropospheric NO_2 columns using the OMI/Aura satellite tropospheric NO_2 product, Atmos. Chem. Phys., 10, 8839–8854, doi:10.5194/acp-10-8839-2010, 2010. 17248

Jerrett, M., Finkelstein, M. M., Brook, J. R., Arain, M. A., Kanaroglou, P., Stieb, D. M., Gilbert, N. L., Verma, D., Finkelstein, N., Chapman, K. R., and Sears, M. R.: A cohort study of traffic-related air pollution and mortality in Toronto, Ontario, Canada, Environ. Health Persp., 117, 772–777, doi:10.1289/ehp.11533, 2009. 17247

ACPD
11, 17245–17287, 2011

Kim, S. W., Heckel, A., Frost, G. J., Richter, A., Gleason, J., Burrows, J. P., McKeen, S., Hsie, E. Y., Granier, C., and Trainer, M.: NO_2 columns in the Western United States observed from space and simulated by a regional chemistry model and their implications for NO_x emissions, J. Geophys. Res., 114, D11301, doi:10.1029/2008JD011343, 2009. 17249

Kramer, L. J., Leigh, R. J., Remedios, J. J., and Monks, P. S.: Comparison of OMI and ground-based in situ and MAX-DOAS measurements of tropospheric nitrogen dioxide in an urban area, J. Geophys. Res.-Atmos., 113, D16S39, doi:10.1029/2007JD009168, 2008. 17248

Lamsal, L. N., Martin, R. V., van Donkelaar, A., Steinbacher, M., Celarier, E. A., Bucsela, E., Dunlea, E. J., and Pinto, J. P.: Ground-level nitrogen dioxide concentrations inferred from the satellite-borne Ozone Monitoring Instrument, J. Geophys. Res.-Atmos., 113, D16308, doi:10.1029/2007JD009235, 2008. 17248, 17250, 17252, 17255, 17256, 17263

Lamsal, L. N., Martin, R. V., van Donkelaar, A., Celarier, E. A., Bucsela, E. J., Boersma, K. F., Dirksen, R., Luo, C., and Wang, Y.: Indirect validation of tropospheric nitrogen dioxide retrieved from the OMI satellite instrument: insight into the seasonal variation of nitrogen oxides at northern midlatitudes, J. Geophys. Res.-Atmos., 115, D05302, doi:10.1029/2009JD013351, 2010. 17248, 17254, 17255, 17259

Lenters, V., Uiterwaal, C. S., Beelen, R., Bots, M. L., Fischer, P., Brunekreef, B., and Hoek, G.: Long-term exposure to air pollution and vascular damage in young adults, Epidemiology, 21, 512–520, doi:10.1097/EDE.0b013e3181dec3a7, 2010. 17247

Levelt, P., van den Oord, G., Dobber, M., Malkki, A., Visser, H., de Vries, J., Stammes, P., Lundell, J., and Saari, H.: The Ozone Monitoring Instrument, IEEE T. Geosci. Remote, 44, 1093–1101, doi:10.1109/TGRS.2006.872333, 2006. 17248, 17254

Levy, I., Makar, P. A., Sills, D., Zhang, J., Hayden, K. L., Mihele, C., Narayan, J., Moran, M. D., Sjostedt, S., and Brook, J.: Unraveling the complex local-scale flows influencing ozone patterns in the southern Great Lakes of North America, Atmos. Chem. Phys., 10, 10895–10915, doi:10.5194/acp-10-10895-2010, 2010. 17249, 17253

Makar, P. A., Gong, W., Mooney, C., Zhang, J., Davignon, D., Samaali, M., Moran, M. D., He, H., Tarasick, D. W., Sills, D., and Chen, J.: Dynamic adjustment of climatological ozone boundary conditions for air-quality forecasts, Atmos. Chem. Phys., 10, 8997–9015, doi:10.5194/acp-10-8997-2010, 2010. 17250, 17253

Martin, R. V., Chance, K., Jacob, D. J., Kurosu, T. P., Spurr, R. J. D., Bucsela, E., Gleason, J. F., Palmer, P. I., Bey, I., Fiore, A. M., Li, Q., Yantosca, R. M., and Koelemeijer, R. B. A.: An improved retrieval of tropospheric nitrogen dioxide from GOME, J. Geophys. Res., 107, 4437,

ACPD
11, 17245–17287, 2011

doi:10.1029/2001JD001027, 2002. 17254
MOE: Air Quality in Ontario 2008 Report, available at: http://www.ene.gov.on.ca/publications/7356e.pdf (last access: August 2010), 2008. 17246
NOAA: Lake Erie Temperature Normals, available at: http://www.erh.noaa.gov/buf/laketemps/lktemp.html (last access: December 2010), 2010. 17264
O'Byrne, G., Martin, R. V., van Donkelaar, A., Joiner, J., and Celarier, E. A.: Surface reflectivity from the Ozone Monitoring Instrument using the Moderate Resolution Imaging Spectroradiometer to eliminate clouds: effects of snow on ultraviolet and visible trace gas retrievals, J. Geophys. Res., 115, D17305, doi:10.1029/2009JD013079, 2010. 17248, 17264
Ordóñez, C., Richter, A., Steinbacher, M., Zellweger, C., Nuss, H., Burrows, J., and Prevot, A.: Comparison of 7 years of satellite-borne and ground-based tropospheric NO_2 measurements around Milan, Italy, J. Geophys. Res.-Atmos., 111, D05310, doi:10.1029/2005JD006305, 2006. 17252
Russell, A. R., Valin, L. C., Bucsela, E. J., Wenig, M. O., and Cohen, R. C.: Space-based constraints on spatial and temporal patterns of NO_x emissions in California, 2005–2008, Environ. Sci. Technol., 44, 3608–3615, doi:10.1021/es903451j, 2010. 17248, 17249
Ryerson, T., Williams, E., and Fehsenfeld, F.: An e?cient photolysis system for fast-response NO_2 measurements, J. Geophys. Res.-Atmos., 105, 26447–26461, 2000. 17247
Statistics Canada: 2006 Census of Canada Census Profiles Marital status, common-law status, families, dwellings, and households Tables: Profile of Marital Status, Common-law Status, Families, Dwellings and Households, for Census Metropolitan Areas and Census Agglomerations, 2006 Census., Tech. rep., Statistics Canada, 2006. 17251
Steinbacher, M., Zellweger, C., Schwarzenbach, B., Bugmann, S., Buchmann, B., Ordonez, C., Prevot, A. S. H., and Hueglin, C.: Nitrogen oxide measurements at rural sites in Switzerland: Bias of conventional measurement techniques, J. Geophys. Res.-Atmos., 112, D11307, doi:10.1029/2006JD007971, 2007. 17247, 17252, 17259
US Census Bureau: Table 1. Annual Estimates of the Population of Metropolitan and Micropolitan Statistical Areas: 1 April 2000 to 1 July 2009 (CBSA-EST2009-01), available at: http://www.census.gov/popest/metro/CBSA-est2009-annual.html (last access: October 2010), 2010. 17251

ACPD
11, 17245–17287, 2011

Table 1. Correlation (Pearson R) between NO_2 measurement sites during the BAQS-met campaign (1 June to 10 September, 2007). The first row for each location represents the correlation between hourly measurements while the second represents correlation between daily measurements. All monitors not marked with a * were heated molybdenum converted chemiluminescence monitors while those marked with a * were photolytically converted chemiluminescence monitors.

Site	Harrow (MoE)	Ridge-town	Windsor West	Windsor Downtown	Chatham	Harrow (EC)*	Bear Creek*
Pelee	0.49 0.54	0.43 0.35	0.51 0.63	0.51 0.60	0.46 0.54	0.41 0.35	0.36 0.43
Harrow (MoE)		0.48 0.51	0.50 0.58	0.49 0.57	0.47 0.41	0.95 0.87	0.46 0.68
Ridgetown			0.71 0.65	0.68 0.68	0.59 0.63	0.42 0.36	0.55 0.76
Windsor West				0.85 0.83	0.56 0.39	0.47 0.41	0.49 0.50
Windsor Downtown					0.63 0.50	0.42 0.32	0.46 0.44
Chatham						0.30 0.17	0.44 0.47
Harrow (EC)*							0.37 0.34

ACPD
11, 17245–17287, 2011

Table 2. Minimum, median and maximum observed 1-day and 1-week average NO_2 concentrations measured by chemiluminescence monitor during the BAQS-met campaign. All monitors not marked with a * were heated molybdenum converted chemiluminescence monitors while those marked with a * were photolytically converted chemiluminescence monitors.

Site	Daily Min (ppb)	Daily Median (ppb)	Daily Max (ppb)	Weekly Min (ppb)	Weekly Median (ppb)	Weekly Max (ppb)
Pelee	0.1	2.8	4.0	1.7	2.9	3.1
Harrow (MoE)	3.1	5.3	8.0	5.3	5.4	5.5
Ridgetown	2.5	5.8	7.1	4.8	5.0	6.0
Windsor West	5.5	13.2	22.9	10.8	12.9	15.2
Windsor Downtown	4.4	13.1	30.6	11.3	13.6	18.6
Chatham	2.2	7.0	13.7	5.6	7.2	7.6
Harrow (EC)*	2.6	4.5	7.9	3.7	4.8	5.4
Bear Creek*	1.1	2.9	6.1	2.4	3.1	4.1

ACPD
11, 17245–17287, 2011

Table 3. Mean surface-to-column ratio (± 95 % confidence interval) and characteristic height, by season.

Season	Mean surface-to-column ratio (± 95 % CI) (ppb/1 × 10^{15} molec cm^{-2})	Mean characteristic height (m)
Winter	2.0 (± 0.41)	210
Spring	1.7 (± 0.13)	245
Summer	0.94 (± 0.07)	450
Autumn	0.81 (± 0.07)	525

ACPD
11, 17245–17287, 2011

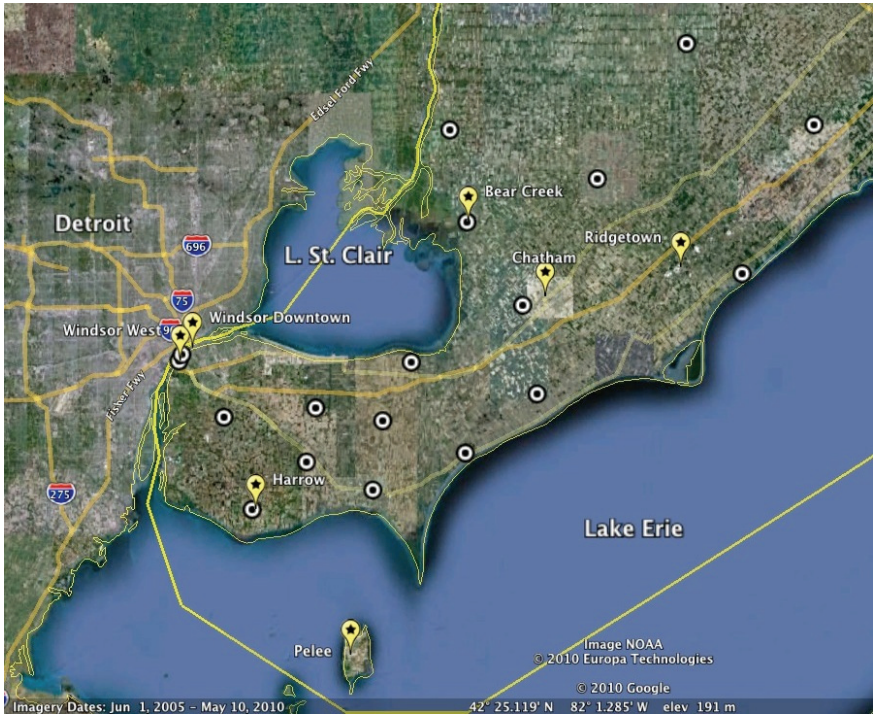

Fig. 1. NO_2 monitoring sites for the 2007 BAQS-Met campaign. Passive monitoring locations are denoted by black-and-white circles. High-time resolution chemiluminescence monitor locations are marked by yellow bubbles with text labels. Chatham, Windsor West and Windsor Downtown were Ontario Ministry of the Environment (MoE) permanent monitoring stations. Harrow, Pelee and Ridgetown also had monitors operated by MoE from 20 June to 10 July. Harrow had a photolytically converted chemiluminescence monitor operated by Environment Canada from 1 June to 10 September and Bear Creek had both molybdenum and photolytically converted monitors operated by Environment Canada for the same period. Two additional MoE permanent monitoring station not shown by this map were also used (Sarnia and London).

ACPD
11, 17245–17287, 2011

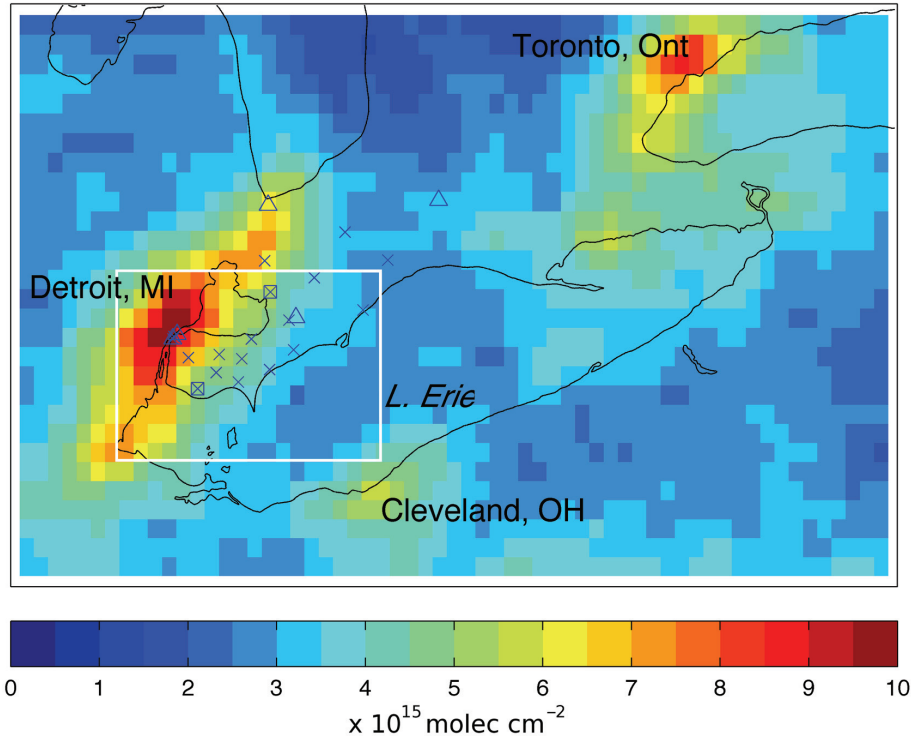

Fig. 2. Campaign average NO_2 column in Southwestern Ontario. BAQS-met passive monitoring sites are marked by Xs, triangles represent permanent MoE molybdenum converted NO_x monitoring locations and squares denote locations of EC photolytically converted NO_x monitors during the campaign. White rectangle outlines area encompassed by Fig. 1.

ACPD
11, 17245–17287, 2011

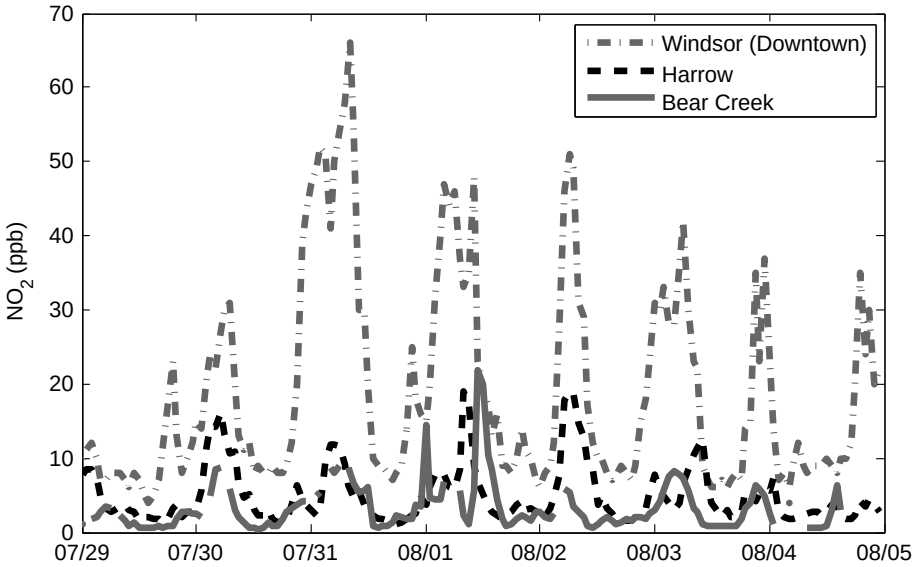

Fig. 3. NO_2 measured at 1 urban (Windsor) and 2 rural (Harrow, Bear Creek) locations during 1 week of the BAQS-met 2007 campaign. This week was selected as generally representative of patterns observed over the whole campaign. NO_2 concentrations can be seen to exhibit significant diurnal and day-to-day variation.

ACPD
11, 17245–17287, 2011

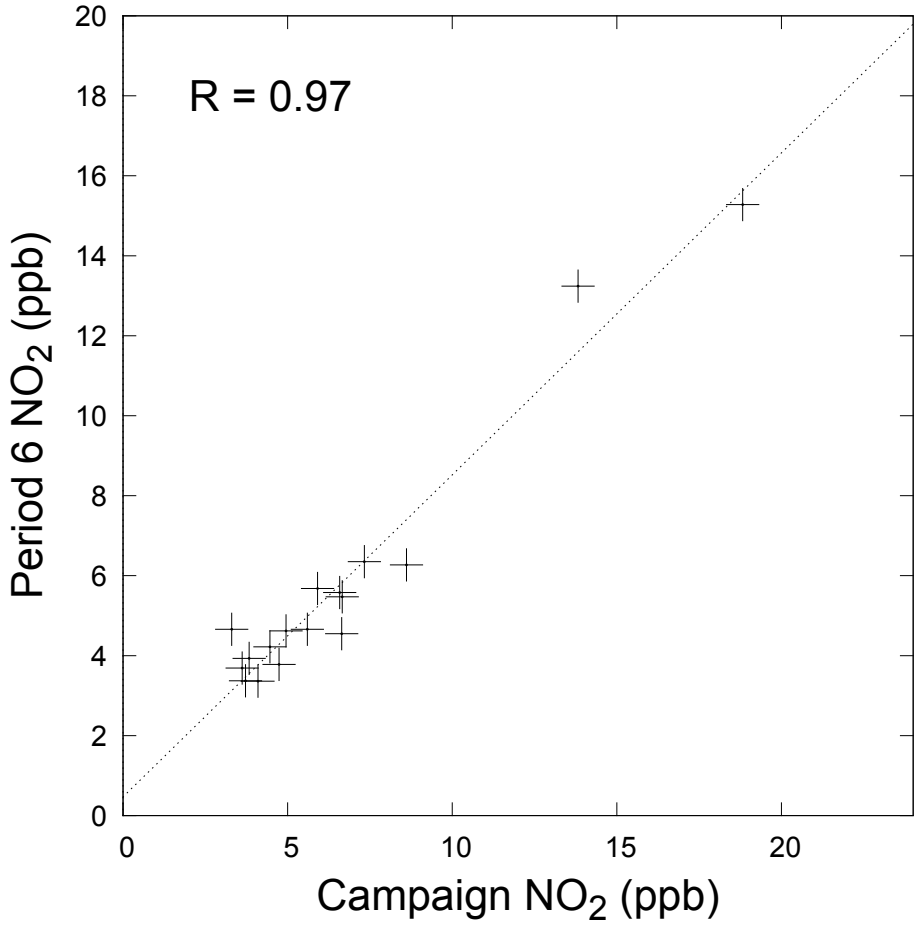

Fig. 4. Single sampling period average NO_2 concentration vs. same-site campaign average concentrations for sampling period 6 (7–21 August). This sampling period represented the lowest linear correlation against the average concentration.

ACPD
11, 17245–17287, 2011

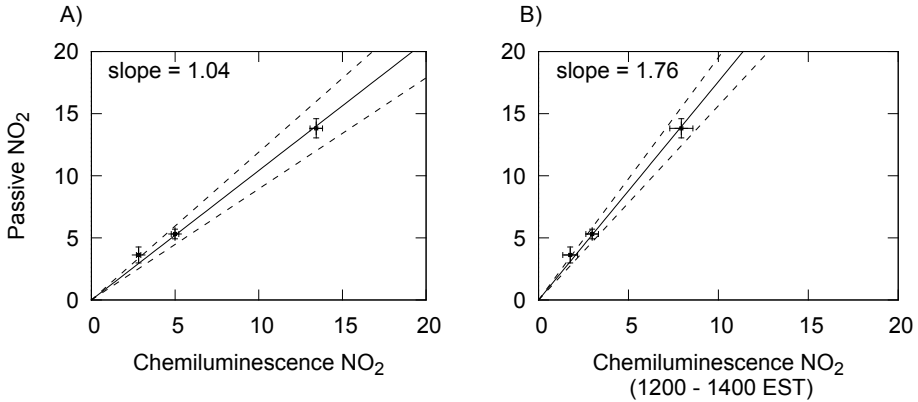

Fig. 5. Comparison of collocated passive and chemiluminescence monitors. *X*-error bars represent 95 % confidence intervals on averages from hourly data. *Y*-error bars represent 95 % confidence intervals on averages from approximately 2-week sampling period data.

ACPD
11, 17245–17287, 2011

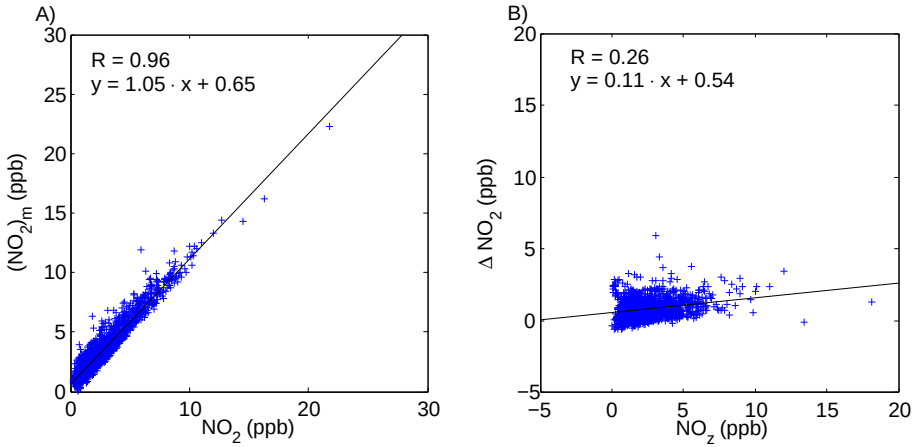

Fig. 6. (A) Comparison of collocated high-time resolution NO_2 measurements made by heated molybdenum converted (vertical axis) and photocatalytically converted (horizontal axis) chemiluminescence monitor. The solid line is the best-fit linear regression. **(B)** Comparison of difference between molybdenum converted and photocatalytic NO_2 measurements with NO_z measurements (taken by BC2 monitor).

ACPD
11, 17245–17287, 2011

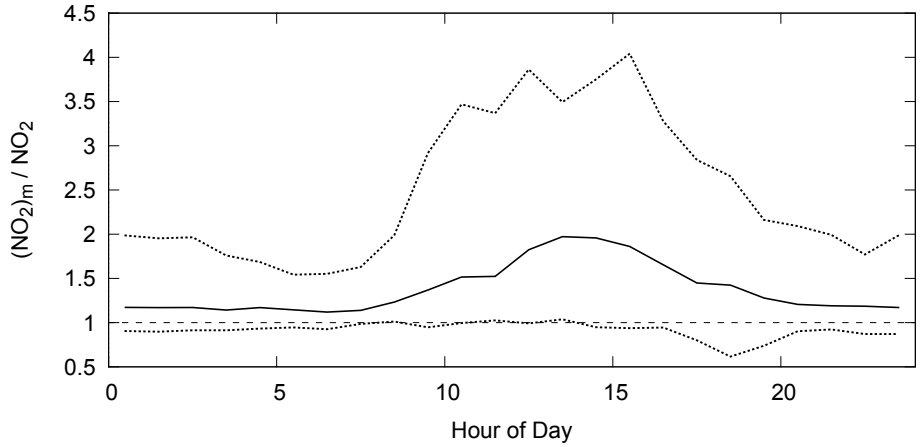

Fig. 7. Diurnal trend in ratio of $(NO_2)_m$ to NO_2 measured from 1 June to 10 September, 2007 at Bear Creek, Ontario, a rural site located approximately 60 km northeast of downtown Detroit, MI. $(NO_2)_m$ denotes NO_2 measured by heated molybdenum catalyst chemiluminescence monitor, which can suffer from interference due to reducing non-NO_2 oxidized nitrogen species. True NO_2 was measured by a collocated photolytic converted chemiluminescence monitor, which reduces NO_2 selectively. Solid line represents median ratio for that hour. Dotted lines represent 5th and 95th percentiles. Hours are Eastern Standard Time. OMI overpasses occur between 12:00 and 14:00 EST, which display some of the highest average ratios.

ACPD
11, 17245–17287, 2011

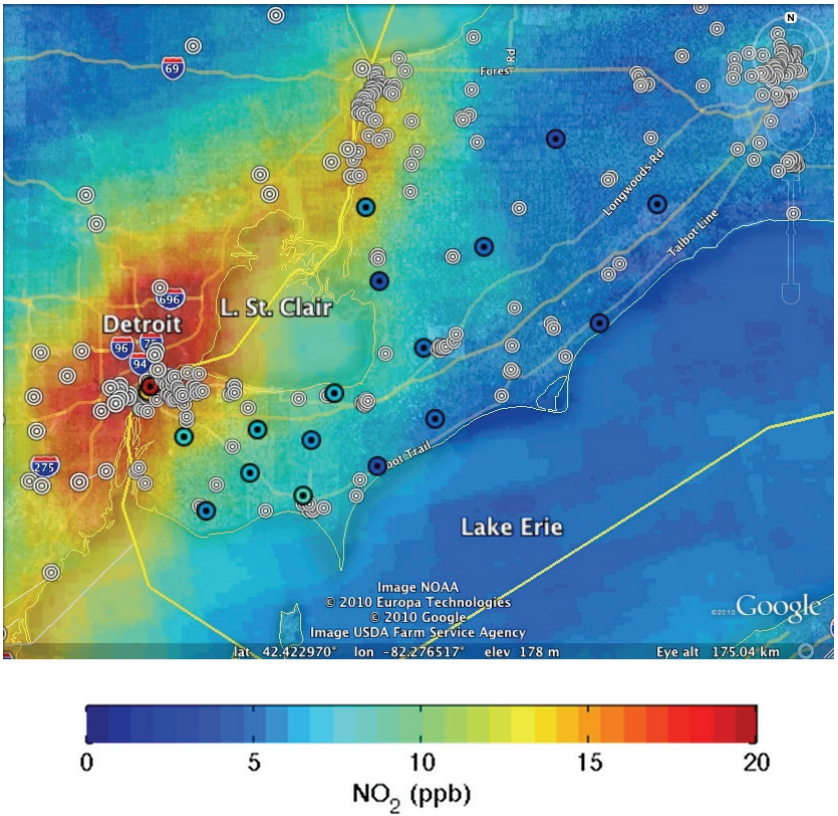

Fig. 8. Map of the campaign area with passive monitoring site campaign averages and emissions sources. False colour indicates OMI-inferred NO_2. The passive sites are marked by coloured circles with the colour of the circle representing the campaign average NO_2 concentration (same scale as false colour map). US EPA emissions sources with 2005 emissions greater than 100 t NO_x/yr are marked on the US side, while Environment Canada NPRI emissions greater than 100 t NO_2/yr are marked.

ACPD
11, 17245–17287, 2011

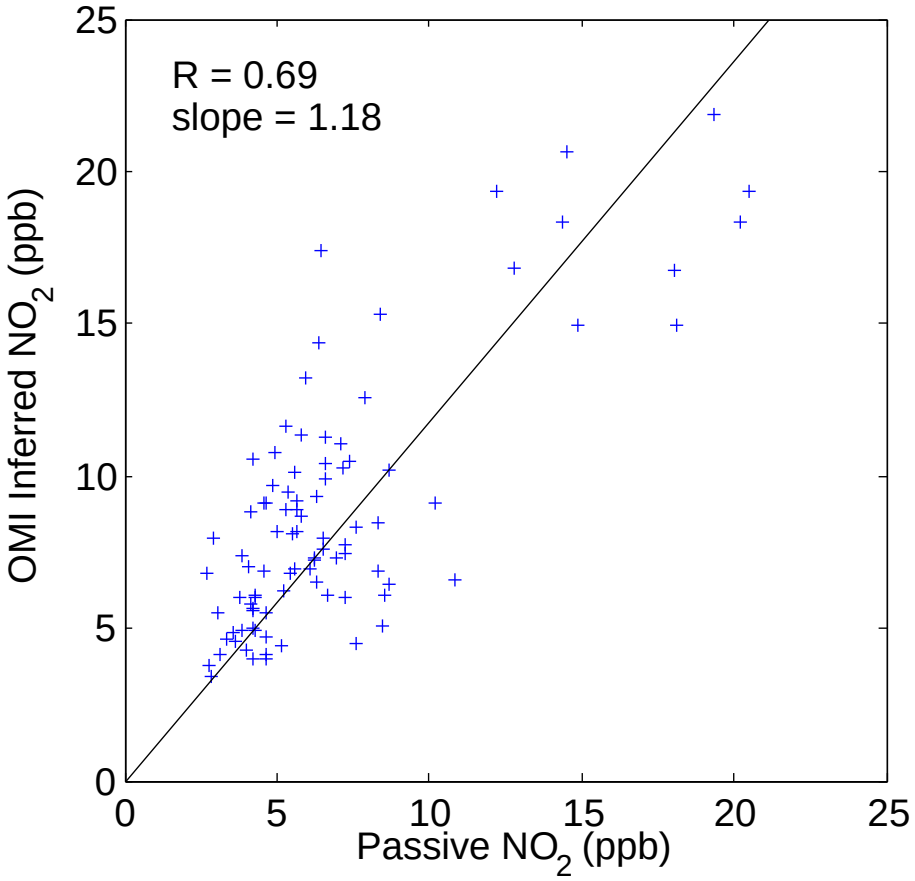

Fig. 9. Passive measurements taken during the BAQS-met campaign over 7 sampling periods at 17 simultaneous locations versus OMI inferred NO_2 concentrations at those same locations for the same periods.

ACPD
11, 17245–17287, 2011

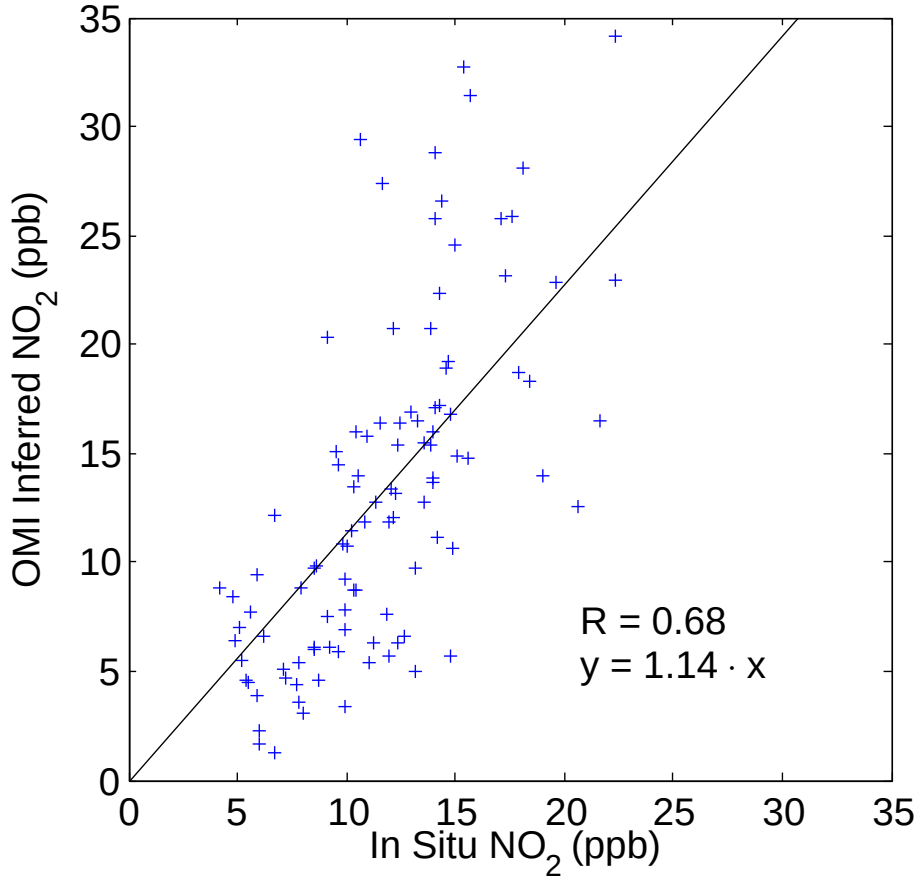

Fig. 10. Two-week average OMI inferred surface NO_2 vs. in situ CL NO_2 measurements for 2005–2009. Improvement in correlation ($R = 0.61$ for DOMINO columns vs. in situ) was mainly due to a few periods in winter months, which showed greater agreement after the inference method was applied.

ACPD
11, 17245–17287, 2011

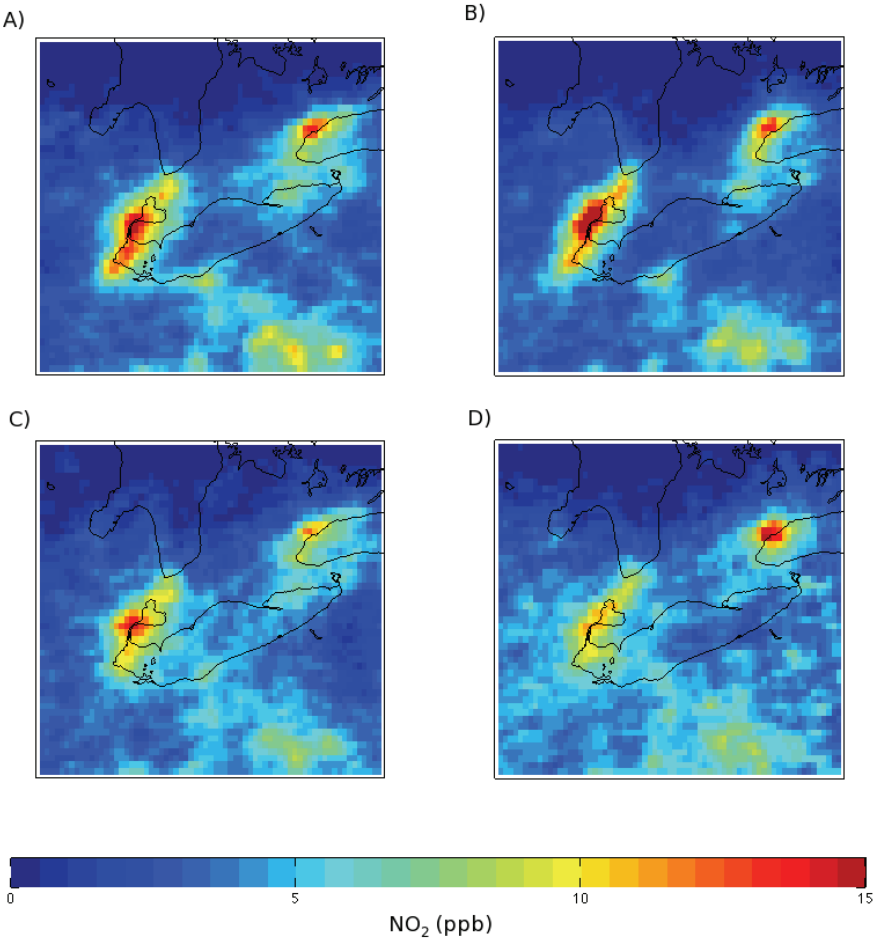

Fig. 11. OMI inferred NO_2 concentrations for summers of **(A)** 2006, **(B)** 2007, **(C)** 2008 and **(D)** 2009.

ACPD
11, 17245–17287, 2011

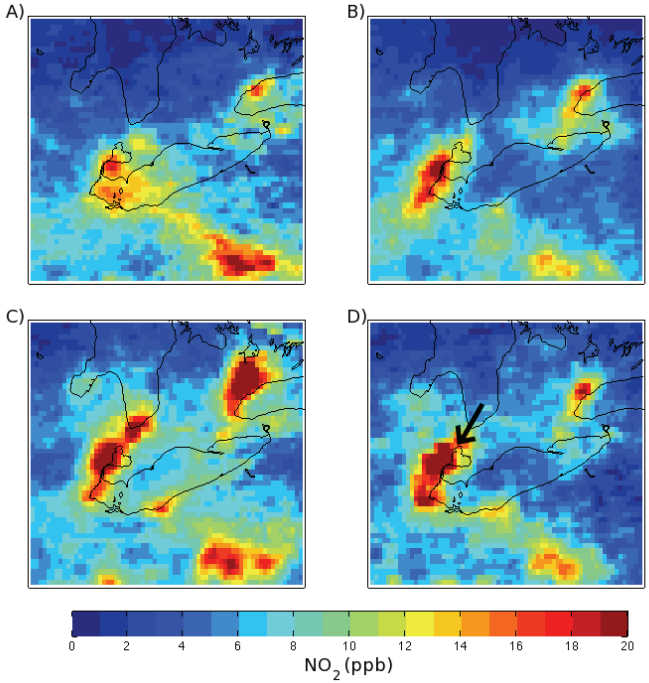

Fig. 12. OMI inferred NO_2 concentrations for 2007 grouped by surface wind direction as measured at Windsor. **(A)** represents only OMI measurements taken when wind was blowing from the NW direction. (**B**, **C** and **D**) Same as **(A)** but NE, SW and SE directions, respectively. NW coast of Lake St. Clair indicated by black arrow in **(D)**; inferred concentrations over the lake are approximately half those onshore when the lake is upwind of the onshore emissions sources (i.e. when the wind blows from the SE). Number of overpasses used to generate each average was 21 (21 % of available overpasses) for **(A)**, 70 for **(B)**, 98 for **(C)** and 48 for **(D)**. The total number of overpasses used is less than the total number of days in the year because of rejection of overpasses for which > 2 surface stations were occluded by clouds.

ACPD
11, 17245–17287, 2011

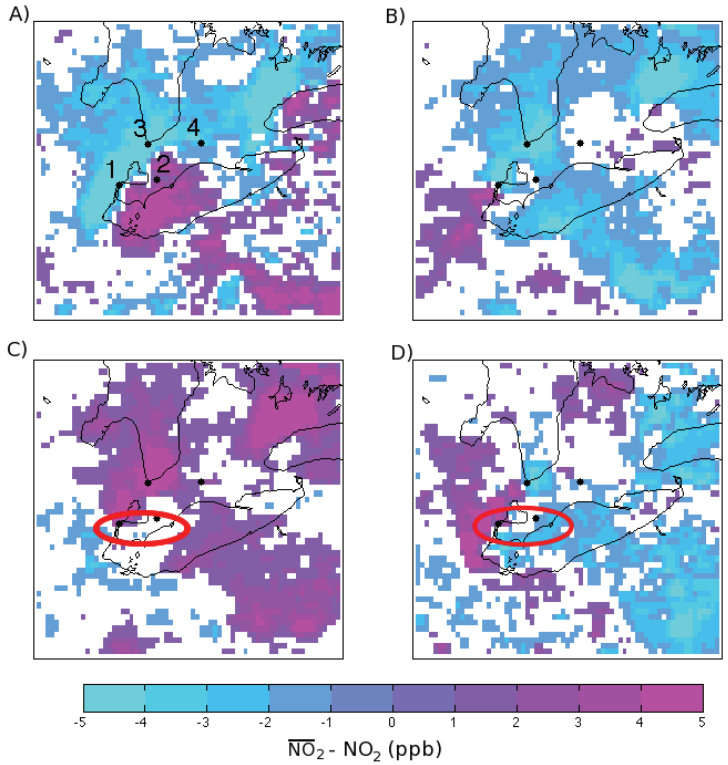

Fig. 13. Difference between OMI inferred NO_2 grouped by wind direction and annual average OMI inferred NO_2. Purple (positive), indicates higher than average NO_2 concentrations when the wind blows from that direction while blue indicates lower than average concentrations. Uncoloured regions are less than 1 ppb Difference. Labeled points in **(A)** represent surface monitoring stations (1: WW and WD; 2: CH; 3: SA; 4: LO) **(A)** represents only OMI measurements taken when wind was blowing from the NW direction. (**B**, **C** and **D**) Same as **(A)** but NE, SW and SE directions, respectively. See text for in-depth description regarding marked areas in **(C)** and **(D)**.

ACPD
11, 17245–17287, 2011